Higher-Order Relaxation Schemes for Hyperbolic Systems of Conservation Laws *

Mapundi K. Banda† and Mohammed Seaïd‡

Fachbereich Mathematik
TU Darmstadt, 64289 Darmstadt, Germany

Abstract

We present a higher order generalisation for relaxation methods in the framework presented by Jin and Xin in [9]. The schemes employ general higher order integration for spatial discretisation and higher order implicit-explicit schemes or Total Variation diminishing (TVD) Runge-Kutta schemes for time integration of relaxed or relaxing schemes, respectively, for time integration. Numerical experiments are performed on various test problems, in particular, the Euler equations of inviscid gas dynamics. In addition, uniform convergence with respect to the relaxation parameter is demonstrated.

Keywords. Relaxation methods, hyperbolic systems, inviscid gas Euler equations, higher order upwind schemes, Runge-Kutta methods

AMS subject classifications. 35L65, 76M12, 65L06, 76P05

1 Introduction

Given an open bounded domain $\Omega \subset \mathbb{R}$ and a time interval $[0, T]$, it is the goal of this paper to construct higher order relaxation schemes for the one dimensional hyperbolic system of conservation laws

$$\begin{aligned} \frac{\partial \mathbf{u}}{\partial t} + \frac{\partial}{\partial x}\mathbf{f}(\mathbf{u}) &= 0, \quad \text{in} \quad \Omega \times (0, T), \\ \mathbf{u}(x, 0) &= \mathbf{u}_0(x), \quad \text{in} \quad \Omega, \end{aligned} \tag{1}$$

*This work was supported by DAAD and DFG grants KL 1105/9-1

†banda@mathematik.tu-darmstadt.de

‡seaid@mathematik.tu-darmstadt.de

where $\mathbf{u} \in \mathbb{R}^m$ and the flux function $\mathbf{f}(\mathbf{u}) : \mathbb{R}^m \to \mathbb{R}^m$ is nonlinear. We apply the relaxation method presented in [9] to problem (1) whereby we obtain a relaxation system of the form:

$$\begin{aligned} \frac{\partial \mathbf{u}}{\partial t} + \frac{\partial \mathbf{v}}{\partial x} &= 0, \\ \frac{\partial \mathbf{v}}{\partial t} + \mathbf{A}^2 \frac{\partial \mathbf{u}}{\partial x} &= -\frac{1}{\tau}\Big(\mathbf{v} - \mathbf{f}(\mathbf{u})\Big), \\ \mathbf{u}(x,0) = \mathbf{u}_0(x), \qquad & \mathbf{v}(x,0) = \mathbf{f}\big(\mathbf{u}_0(x)\big), \end{aligned} \tag{2}$$

where $\mathbf{v} \in \mathbb{R}^m$, $\mathbf{A}^2 := \mathrm{diag}\big(a_1^2, \ldots, a_m^2\big) \in \mathbb{R}^{m\times m}$ and τ is the relaxation rate. The relaxation system (2) has a typical semilinear structure with the two linear characteristic variables

$$\mathbf{v} + \mathbf{A}\mathbf{u} \qquad \text{and} \qquad \mathbf{v} - \mathbf{A}\mathbf{u}. \tag{3}$$

Hence we have replaced a nonlinear system by a semi-linear system with the main advantage that it can be solved numerically without introducing Riemann solvers. Moreover, it has been shown analytically, see for example [4, 14, 16, 17], that solutions to (2) approach solutions to the original problem (1) if the subcharacteristic condition

$$\frac{|\lambda|}{a_i} \leq 1, \qquad i = 1, \ldots m, \tag{4}$$

is satisfied for every eigenvalue λ of $\mathbf{f}'(\mathbf{u})$.

The relaxation schemes as defined above were first introduced in [9]. There a first order upwind scheme and a second order MUSCL scheme was used for the space discretization and second order implicit-explicit TVD Runge-Kutta scheme for the time integration. See also other approaches in [5, 7, 11, 20] and the references cited therein. In [9] second order schemes were developed. In this paper we follow the same idea and extend it to higher order. A rigorous derivation of the higher order schemes will be presented as well as their numerical efficiency.

In this paper, we discuss only the one-dimensional systems of hyperbolic conservation laws. As part of an ongoing project, this study will be extended to multi-dimensional problems in several space variables and problems with forcing terms, especially Boltzmann and Navier-Stokes models [3]. The rest of the paper is organized as follows: Section 2 presents an overview of the basic ideas of relaxation schemes, special attention is paid to the first and second order schemes. Section 3 is devoted to the construction of high order relaxation schemes with a more detailed formulation of a third order scheme. Numerical results for the Euler equations of gas dynamics are reported in Section 4. Section 5 contains concluding remarks.

2 The Relaxation Schemes: A Brief Overview

Relaxation schemes are in fact a combination of non-oscillatory upwind space discretization and a TVD implicit-explicit time integration of the resulting semi-discrete system, see for instance [9, 16, 17]. The fully discrete system of the equations (2) is referred to as a relaxing system while that of the limiting system as the relaxation rate tends to zero, $\tau \to 0$, is called a relaxed scheme.

To discretize the system of equations (2) we assume, for simplicity, an equally spaced grid with grid space $\Delta x := x_{i+\frac{1}{2}} - x_{i-\frac{1}{2}}$ and a uniform time step $\Delta t := t_{n+1} - t_n$. We use the notation $\omega^n_{i+\frac{1}{2}} := \omega(x_{i+\frac{1}{2}}, t_n)$ and

$$\omega^n_i := \frac{1}{\Delta x}\int_{x_{i-\frac{1}{2}}}^{x_{i+\frac{1}{2}}} \omega(x, t_n)dx,$$

to denote the point-value and the approximate cell-average of the function ω at $x = x_{i+\frac{1}{2}}$, $t = t_n$; and $x = x_i$, $t = t_n$, respectively.

We define the following difference operator

$$\mathcal{D}_x \omega_i := \frac{\omega_{i+\frac{1}{2}} - \omega_{i-\frac{1}{2}}}{\Delta x}. \tag{5}$$

Then, a semi-discrete approximation for the system of equations (2) can be written as

$$\begin{aligned} \frac{d\mathbf{u}_i}{dt} + \mathcal{D}_x \mathbf{v}_i &= 0, \\ \frac{d\mathbf{v}_i}{dt} + \mathbf{A}^2 \mathcal{D}_x \mathbf{u}_i &= -\frac{1}{\tau}\Big(\mathbf{v}_i - \mathbf{f}(\mathbf{u}_i)\Big). \end{aligned} \tag{6}$$

Notice that, the space and time discretizations are treated separately using the method of lines. Any approximation for the numerical fluxes in (5) should be accompanied by an ODE solver for (6) of the same order of accuracy. In this section we give a brief overview of the first and second order relaxing systems as presented in [9].

2.1 First Order Relaxation Scheme

A first order upwind scheme is applied to the characteristic variables (3) in order to obtain the numerical fluxes in (5) for the k-th component by

$$(v + a_k u)_{i+\frac{1}{2}} = (v + a_k u)_i, \qquad (v - a_k u)_{i+\frac{1}{2}} = (v - a_k u)_{i+1}.$$

to obtain

$$\begin{aligned} u_{i+\frac{1}{2}} &:= \frac{u_i + u_{i+1}}{2} - \frac{v_{i+1} - v_i}{2a_k}, \\ v_{i+\frac{1}{2}} &:= \frac{v_i + v_{i+1}}{2} - a_k \frac{u_{i+1} - u_i}{2}. \end{aligned} \tag{7}$$

To integrate in time the equations (6) we propose a first order implicit-explicit splitting given by the usual Butcher tables

$$\begin{array}{c|c} 0 & 0 \\ \hline & 1 \end{array} \qquad \begin{array}{c|c} 1 & 1 \\ \hline & 1 \end{array} \tag{8}$$

where the left and right tables represent the explicit and implicit Runge-Kutta schemes, respectively. Hence, the implementation of the first order relaxation algorithm to solve (1) is carried out in simple steps as follows:

Given $\{u_i^n, v_i^n\}$, $\{u_i^{n+1}, v_i^{n+1}\}$ are computed by

$$\begin{aligned}
u_i^* &= u_i^n, \\
v_i^* &= v_i^n - \frac{\Delta t}{\tau}\left(v_i^* - \mathbf{f}(u_i^*)\right); \\
u_i^{(1)} &= u_i^* - \Delta t \mathcal{D}_x v_i^*, \\
v_i^{(1)} &= v_i^* - \Delta t \mathbf{A}^2 \mathcal{D}_x u_i^*; \\
u_i^{n+1} &= u_i^{(1)}, \\
v_i^{n+1} &= v_i^{(1)}.
\end{aligned} \tag{9}$$

When $\tau \longrightarrow 0$, equations (9) reduce to the so called relaxed scheme

$$\begin{aligned}
u_i^{(1)} &= u_i^n - \Delta t \mathcal{D}_x v_i^n \Big|_{v_i^n = \mathbf{f}(u_i^n)}, \\
u_i^{n+1} &= u_i^{(1)}.
\end{aligned} \tag{10}$$

Note that, the relaxed scheme (10) is the first order explicit scheme given by the left table in (8), applied to the original system (1). The difference operator $\mathcal{D}_x$ is defined as in (5) by projecting the numerical flux $v_{i+\frac{1}{2}}$ into the local equilibrium $\mathbf{f}_{i+\frac{1}{2}} := \mathbf{f}(u_{i+\frac{1}{2}})$ using (7). A similar scheme has also been attributed to Rusanov in [13].

2.2 Second Order Relaxation Scheme

For the second order scheme, we use the MUSCL method presented in [19] for the discretization along the characteristic variables (3). This method yields to the semi-discrete system (6), where the numerical fluxes for, the k-th component are

$$\begin{aligned}
u_{i+\frac{1}{2}} &:= \frac{u_i + u_{i+1}}{2} - \frac{v_{i+1} - v_i}{2a_k} + \frac{\sigma_i^+ + \sigma_{i+1}^-}{4a_k}, \\
v_{i+\frac{1}{2}} &:= \frac{v_i + v_{i+1}}{2} - a_k \frac{u_{i+1} - u_i}{2} + \frac{\sigma_i^+ - \sigma_{i+1}^-}{4}.
\end{aligned} \tag{11}$$

We use Sweby's notation to define the slopes of $v \pm a_k u$ by

$$\begin{aligned}
\sigma_i^\pm &= \left(v_{i+1} \pm a_k u_{i+1} - v_i \mp a_k u_i\right)\phi(\theta_i^\pm), \\
\theta_i^\pm &= \frac{v_i \pm a_k u_i - v_{i-1} \mp a_k u_{i-1}}{v_{i+1} \pm a_k u_{i+1} - v_i \mp a_k u_i}.
\end{aligned}$$

and ϕ is a slope limiter function. The simplest choice of a slope limiter is the so-called minmod limiter,

$$\phi(\theta) = \max(0, \min(1, \theta)).$$

A sharper Van-Leer limiter may also be used which is given by [19],

$$\phi(\theta) = \frac{|\theta| + \theta}{1 + |\theta|}.$$

Note that if we set the slopes $\sigma_i^{\pm} = 0$ or $\phi = 0$, the equations (11) reduce to the first order scheme (7).

With a similar piecewise implicit-explicit reconstruction as before, we introduce the second order TVD Runge-Kuta scheme presented in [10]. Its corresponding Butcher double tables are

$$\begin{array}{c|cc} 0 & 0 & 0 \\ 1 & 1 & 0 \\ \hline & \frac{1}{2} & \frac{1}{2} \end{array} \qquad \begin{array}{c|cc} -1 & -1 & 0 \\ 2 & 1 & 1 \\ \hline & \frac{1}{2} & \frac{1}{2} \end{array} \tag{12}$$

Consequently, we can formulate the second order relaxation scheme to integrate (2) as follows: Given $\{u_i^n, v_i^n\}$, $\{u_i^{n+1}, v_i^{n+1}\}$ are computed by

$$\begin{aligned} u_i^* &= u_i^n, \\ v_i^* &= v_i^n + \frac{\Delta t}{\tau}\Big(v_i^* - \mathbf{f}(u_i^*)\Big); \\ u_i^{(1)} &= u_i^* - \Delta t \mathcal{D}_x v_i^*, \\ v_i^{(1)} &= v_i^* - \Delta t \mathbf{A}^2 \mathcal{D}_x u_i^*; \\ u_i^{**} &= u_i^{(1)}, \\ v_i^{**} &= v_i^{(1)} - \frac{\Delta t}{\tau}\Big(v_i^{**} - \mathbf{f}(u_i^{**})\Big) - \frac{2\Delta t}{\tau}\Big(v_i^* - \mathbf{f}(u_i^*)\Big); \\ u_i^{(2)} &= u_i^{**} - \Delta t \mathcal{D}_x v_i^{**}, \\ v_i^{(2)} &= v_i^{**} - \Delta t \mathbf{A}^2 \mathcal{D}_x u_i^{**}; \\ u_i^{n+1} &= \frac{1}{2}(u_i^n + u_i^{(2)}), \\ v_i^{n+1} &= \frac{1}{2}(v_i^n + v_i^{(2)}). \end{aligned} \tag{13}$$

It was shown in [9], the variables v_i^* and v_i^{**} in (13) approximate the local equilibrium $\mathbf{f}(u_i^*)$ and $\mathbf{f}(u_i^{**})$, respectively when $\tau \longrightarrow 0$. Therefore, a second order relaxed scheme is obtained, based on the left explicit table in (12), as

$$\begin{aligned} u_i^{(1)} &= u_i^n - \Delta t \mathcal{D}_x v_i^n \Big|_{v_i^n = \mathbf{f}(u_i^n)}, \\ u_i^{(2)} &= u_i^{(1)} - \Delta t \mathcal{D}_x v_i^{(1)} \Big|_{v_i^{(1)} = \mathbf{f}(u_i^{(1)})}, \\ u_i^{n+1} &= \frac{1}{2}(u_i^n + u_i^{(2)}). \end{aligned} \tag{14}$$

It is worth remarking that, using these schemes neither linear algebraic equation nor nonlinear source terms can arise. In addition both first and second order relaxation schemes are stable independent of τ, so that the choice of Δt is based only on the usual CFL condition

$$\mathrm{CFL} := \max_i a_i \frac{\Delta t}{\Delta x} \leq 1. \tag{15}$$

Note also that the time-discretisation in the limit when $\tau \longrightarrow 0$ converges to the TVD Runge-Kutta schemes given by Shu and Osher in [6], also referred to as Strong Stability-Preserving (SSP) Time Discretisation Methods in [8]. We further remark that different choices of $a_k, k \in \{1, \ldots, m\}$ can be taken. In [9] several choices have been highlighted. Other plausible choices have been used in the numerical experiments in this paper and will be discussed below.

3 Extension to Third- and Higher-Order.

In this section we generalise the relaxation schemes so that higher order schemes can be used. The idea is to define an interpolating polynomial which is used in the MUSCL-type formulation above. Using this formulation the fluxes at the cell boundaries can be derived.

To generalise the Relaxation Schemes we will first modify our notation slightly: Using the discretisation introduced in Section 2 we consider a cell in the domain Ω which we denote $\mathcal{I}_i = [x_{i-\frac{1}{2}}, x_{i+\frac{1}{2}}]$ containing the gridpoint x_i . We denote an interpolating polynomial defined on cell $\mathcal{I}_i$ by $p_i(x,t)$. Thus the k-th component of the solution is reconstructed by piecewise polynomials as:

$$u_k(x,t) = \sum_i p_i(x,t;\mathbf{u})\chi_i(x). \tag{16}$$

where χ_i is a characteristic polynomial defined on cell $\mathcal{I}_i$. The values of u_k at the cell boundary point between cells $\mathcal{I}_i$ and $\mathcal{I}_{i+1}$, $x_{i+\frac{1}{2}}$, are denoted as:

$$u_k^+(x_{i+\frac{1}{2}};\mathbf{u}) = p_{i+1}(x_{i+\frac{1}{2}};\mathbf{u}) \qquad \text{and} \qquad u_k^-(x_{i+\frac{1}{2}};\mathbf{u}) = p_i(x_{i+\frac{1}{2}};\mathbf{u}).$$

Now and henceforth, the subscript k will be dropped. It is clear that in the first and second order schemes presented above the following reconstructions were used:

$$\begin{aligned} p_i(x;\mathbf{u}) &= u_i, \\ p_i(x;\mathbf{u}) &= u_i + (u_x)_i(x - x_i), \end{aligned}$$

where u_x is the slope of u. The reconstruction at $x_{i-\frac{1}{2}}$ is defined analogously.

Using this description it is possible to define higher order relaxation schemes using higher order reconstructions. For the presentation of this scheme here the Central Weighted Essentially Non-Oscillatory (CWENO) reconstruction in

[12] which is also the Compact Central Scheme reconstruction [15] will be used. Other reconstructions have been used but the results thereof will not be reported here.

The CWENO reconstruction is defined as below, for more details refer to [12, 15]. Let

$$p_i(x;\mathbf{u}) = w_L P_L(x) + w_R P_R(x) + w_C P_C(x), \tag{17}$$

where

$$w_l = \frac{\alpha_l}{\sum_j \alpha_j}, \quad l,j \in \{L,R,C\}, \qquad \sum_l w_l = 1, \qquad \alpha_l = \frac{c_l}{(\varepsilon + IS_l)^p},$$

$$c_L = c_R = \frac{1}{4}, \qquad c_C = \frac{1}{2}, \qquad IS_L = (u_i - u_{i-1})^2, \qquad IS_R = (u_{i+1} - u_i)^2,$$

$$IS_C = \frac{13}{3}(u_{i+1} - 2u_i + u_{i-1})^2 + \frac{1}{4}(u_{i+1} - u_{i-1})^2,$$

$$P_L(x) = u_i + \frac{u_i - u_{i-1}}{\Delta x}(x - x_i), \qquad P_R(x) = u_i + \frac{u_{i+1} - u_i}{\Delta x}(x - x_i),$$

$$\begin{aligned} P_C(x) \quad &= \quad u_i - \frac{1}{12}(u_{i+1} - 2u_i + u_{i-1}) + \frac{u_{i+1} - u_{i-1}}{2\Delta x}(x - x_i) + \\ &\quad \frac{(u_{i+1} - 2u_i + u_{i-1})}{(\Delta x)^2}(x - x_i)^2. \end{aligned}$$

The constant ε guarantees that the denominator does not vanish and is empirically taken to be 10^{-6} [15]. Likewise the value of p is chosen to provide the highest accuracy in smooth areas and ensure the non-oscillatory nature of the solution near the discontinuities and is selected to be $p = 2$.

With this background we can now reconstruct the characteristic variables as follows:

$$\begin{aligned} (v + au)_{i+\frac{1}{2}} &= (v + au)^-_{i+\frac{1}{2}} = p_i(x_{i+\frac{1}{2}}; \mathbf{v} + a\mathbf{u}), \\ (v - au)_{i+\frac{1}{2}} &= (v - au)^+_{i+\frac{1}{2}} = p_{i+1}(x_{i+\frac{1}{2}}; \mathbf{v} - a\mathbf{u}). \end{aligned}$$

Hence:

$$\begin{aligned} u_{i+\frac{1}{2}} &= \frac{1}{2a}\Big(p_i(x_{i+\frac{1}{2}}; \mathbf{v} + a\mathbf{u}) - p_{i+1}(x_{i+\frac{1}{2}}; \mathbf{v} - a\mathbf{u})\Big), \\ v_{i+\frac{1}{2}} &= \frac{1}{2}\Big(p_i(x_{i+\frac{1}{2}}; \mathbf{v} + a\mathbf{u}) + p_{i+1}(x_{i+\frac{1}{2}}; \mathbf{v} - a\mathbf{u})\Big). \end{aligned}$$

For completeness we write down the explicit expressions of the flux variables below:

$$
\begin{aligned}
v_{i+\frac{1}{2}} &= \frac{1}{2}\Big(p_i(x_{i+\frac{1}{2}};\mathbf{v}+a\mathbf{u}) + p_{i+1}(x_{i+\frac{1}{2}};\mathbf{v}-a\mathbf{u})\Big) \\
&= \frac{1}{2}\Bigg\{ w_L^+\Big[(v+au)_i + \frac{1}{2}\Big((v+au)_i - (v+au)_{i-1}\Big)\Big] + \\
&\quad w_R^+\Big[(v+au)_i + \frac{1}{2}\Big((v+au)_{i+1} - (v+au)_i\Big)\Big] + \\
&\quad w_C^+\Big[(v+au)_i - \frac{1}{12}\Big((v+au)_{i+1} - 2(v+au)_i + (v+au)_{i-1}\Big) + \\
&\quad \frac{1}{4}\Big((v+au)_{i+1} - (v+au)_{i-1}\Big) + \\
&\quad \frac{1}{4}\Big((v+au)_{i+1} - 2(v+au)_i + (v+au)_{i-1}\Big)\Big] + \\
&\quad w_L^-\Big[(v-au)_{i+1} + \frac{1}{2}\Big((v-au)_{i+1} - (v-au)_i\Big)\Big] + \\
&\quad w_R^-\Big[(v-au)_{i+1} + \frac{1}{2}\Big((v-au)_{i+2} - (v-au)_{i+1}\Big)\Big] + \\
&\quad w_C^-\Big[(v-au)_{i+1} - \frac{1}{12}\Big((v-au)_{i+2} - 2(v-au)_{i+1} + (v-au)_i\Big) + \\
&\quad \frac{1}{4}\Big((v-au)_{i+2} - (v-au)_i\Big) + \\
&\quad \frac{1}{4}\Big((v-au)_{i+2} - 2(v-au)_{i+1} + (v-au)_i\Big)\Big]\Bigg\},
\end{aligned}
$$

where

$$
w_l^\pm = \frac{\alpha_l^\pm}{\sum_j \alpha_j^\pm}, \quad l,j \in \{L,R,C\}, \qquad \sum_l w_l^\pm = 1, \qquad \alpha_l^\pm = \frac{c_l}{(\varepsilon + IS_l)^p},
$$

$$
c_L = c_R = \frac{1}{4}, \qquad c_C = \frac{1}{2}
$$

$$
IS_L^\pm = \Big((v\pm au)_i - (v\pm au)_{i-1}\Big)^2, \quad IS_R^\pm = \Big((v\pm au)_{i+1} - (v\pm au)_i\Big)^2
$$

$$
\begin{aligned}
IS_C^\pm &= \frac{13}{3}\Big((v\pm au)_{i+1} - 2(v\pm au)_i + (v\pm au)_{i-1}\Big)^2 + \\
&\quad \frac{1}{4}\Big((v\pm au)_{i+1} - (v\pm au)_{i-1}\Big)^2.
\end{aligned}
$$

The expression for $u_{i+\frac{1}{2}}$ can be derived analogously. Therefore, we obtain the following expressions for $u_{i+\frac{1}{2}}$ and analogously for $v_{i+\frac{1}{2}}$:

$$
\begin{aligned}
u_{i+\frac{1}{2}} &:= \frac{u_i + u_{i+1}}{2} - \frac{v_{i+1} - v_i}{2a_k} + \frac{\sigma_i^+ + \sigma_{i+1}^-}{4a_k}, \\
v_{i+\frac{1}{2}} &:= \frac{v_i + v_{i+1}}{2} - a_k\frac{u_{i+1} - u_i}{2} + \frac{\sigma_i^+ - \sigma_{i+1}^-}{4},
\end{aligned}
$$

where

$$
\begin{aligned}
\sigma_i^{\pm} \;=\;& w_L^{\pm}\Big((v \pm au)_i - (v \pm au)_{i-1}\Big) + w_R^{\pm}\Big((v \pm au)_{i+1} - (v \pm au)_i\Big) + \\
& \frac{w_C^{\pm}}{2}\Big((v \pm au)_{i+1} - (v \pm au)_{i-1}\Big) + \\
& \frac{w_C^{\pm}}{3}\Big((v \pm au)_{i+1} - 2(v \pm au)_i + (v \pm au)_{i-1}\Big)
\end{aligned}
$$

We close by pointing out that in this higher order scheme we approximate $f(u)_i$ using the fourth-order Simpson quadrature rule as opposed to the Midpoint Rule which was used in the first and second order cases i.e.

$$
\mathbf{f}(u)_i = \frac{1}{6}\Big[\mathbf{f}(u_{i+\frac{1}{2}}) + 4\mathbf{f}(u_i) + \mathbf{f}(u_{i-\frac{1}{2}})\Big],
$$

where the reconstruction given above is used:

$$
u_{i+\frac{1}{2}} = u^-_{i+\frac{1}{2}}, \qquad u_i = p_i(x_i; \mathbf{u}), \qquad u_{i-\frac{1}{2}} = u^+_{i-\frac{1}{2}}.
$$

Thus for the CWENO reconstruction we obtain the following approximations:

$$
\begin{aligned}
u_{i+\frac{1}{2}} &= w_L P_L(x_{i+\frac{1}{2}}) + w_R P_R(x_{i+\frac{1}{2}}) + w_C P_C(x_{i+\frac{1}{2}}), \\
u_i &= w_L P_L(x_i) + w_R P_R(x_i) + w_C P_C(x_i), \\
u_{i-\frac{1}{2}} &= w_L P_L(x_{i-\frac{1}{2}}) + w_R P_R(x_{i-\frac{1}{2}}) + w_C P_C(x_{i-\frac{1}{2}}),
\end{aligned}
\tag{18}
$$

with the corresponding weights, w_L, w_R, w_C of the polynomials defined accordingly.

The time integration of the space discretized equations is accomplished by third order Runge-Kutta splitting developed in [2, 18], the associated explicit and implicit Butcher tables are

$$
\begin{array}{c|ccccc}
0 & 0 & 0 & 0 & 0 & 0 \\
\frac{1}{2} & \frac{1}{2} & 0 & 0 & 0 & 0 \\
\frac{2}{3} & \frac{11}{18} & \frac{1}{18} & 0 & 0 & 0 \\
\frac{1}{2} & \frac{5}{6} & -\frac{5}{6} & \frac{1}{2} & 0 & 0 \\
1 & \frac{1}{4} & \frac{7}{4} & \frac{3}{4} & -\frac{7}{4} & 0 \\
\hline
 & \frac{1}{4} & \frac{7}{4} & \frac{3}{4} & -\frac{7}{4} & 0
\end{array}
\qquad
\begin{array}{c|ccccc}
0 & 0 & 0 & 0 & 0 & 0 \\
\frac{1}{2} & 0 & \frac{1}{2} & 0 & 0 & 0 \\
\frac{2}{3} & 0 & \frac{1}{6} & \frac{1}{2} & 0 & 0 \\
\frac{1}{2} & 0 & -\frac{1}{2} & \frac{1}{2} & \frac{1}{2} & 0 \\
1 & 0 & \frac{3}{2} & -\frac{3}{2} & \frac{1}{2} & \frac{1}{2} \\
\hline
 & 0 & \frac{3}{2} & -\frac{3}{2} & \frac{1}{2} & \frac{1}{2}
\end{array}
\tag{19}
$$

This procedure can be easily formulated similarly as in (9) and (13). Moreover, as in the case of first and second order schemes, this third order scheme is stable independently of τ under the CFL condition (15).

Obviously, when $\tau \longrightarrow 0$, this scheme leads to the relaxed scheme for the limit equations, which is based on the explicit table in (19).

4 Numerical Examples

In this section we perform some numerical tests with our schemes. We first of all perform tests on a linear problem for accuracy tests. We will consider the relaxed scheme and the relaxing scheme separately. Thereafter we consider the system of Euler equations describing the flow of an inviscid, compressible fluid.

Table 1: Error-norms for the linear advection problem (20) at $t = 1$ using relaxation schemes.

N	Scheme	L^∞-error	Rate	L^1-error	Rate
40	1^{st} order	0.06315	—–	0.06047	—–
	2^{nd} order	0.04173	—–	0.03512	—–
	3^{rd} order	0.06217	—–	0.03346	—–
80	1^{st} order	0.03360	0.91	0.03218	0.91
	2^{nd} order	0.01919	1.12	0.01507	1.22
	3^{rd} order	0.02650	1.23	0.00836	2.00
160	1^{st} order	0.01998	0.75	0.01620	0.99
	2^{nd} order	0.00877	1.13	0.00454	1.73
	3^{rd} order	0.00930	1.51	0.00180	2.21
320	1^{st} order	0.00992	1.01	0.00720	1.17
	2^{nd} order	0.00219	2.00	0.00093	2.28
	3^{rd} order	0.00143	2.70	0.00016	3.46

4.1 One-Dimensional Scalar Linear Hyperbolic Equation

Consider the scalar linear hyperbolic equation

$$u_t + u_x = 0,\ x \in [0, 2\pi], \tag{20}$$

augmented with the initial data, $u(x, 0) = \sin x$, and periodic boundary conditions. This problem admits a global classical solution, which was computed at time $t = 1$ with a varying number of grid points, N.

The associated relaxation system to (20) is constructed as in (2). We choose $a = 1$ and $\tau = 10^{-8}$ in all the computations. In Table 1 we display the errors at $t = 1$ measured in terms of L^∞- and L^1- norms by the difference between the pointvalues of the exact solution and the reconstructed pointvalues of the computed solution. Table 2 shows similar results for the relaxed schemes. We obtain the expected order of accuracy in both L^∞- and L^1- norms. These results demonstrate clearly the numerical convergence of the relaxation schemes to the relaxed schemes as $\tau \longrightarrow 0$ for this example.

Table 2: Error-norms for the linear advection problem (20) at $t = 1$ using relaxed schemes.

N	Scheme	L^∞-error	Rate	L^1-error	Rate
	1st order	0.05923	—	0.05370	—
40	2nd order	0.03271	—	0.02913	—
	3rd order	0.05432	—	0.02531	—
	1st order	0.03196	0.89	0.02779	0.95
80	2nd order	0.01443	1.18	0.01207	1.27
	3rd order	0.02190	1.31	0.00624	2.02
	1st order	0.01631	0.97	0.01370	1.02
160	2nd order	0.00574	1.33	0.00314	1.94
	3rd order	0.00678	1.69	0.00126	2.30
	1st order	0.00793	1.04	0.00541	1.34
320	2nd order	0.00142	2.01	0.00057	2.45
	3rd order	0.00088	2.94	0.00010	3.61

4.2 One-Dimensional Scalar Hyperbolic conservation Laws

In this example we consider solutions to the inviscid Burger's Equation,

$$u_t + (\frac{u^2}{2})_x = 0,\ x \in [0, 2\pi], \tag{21}$$

augmented with the smooth initial data, $u(x, 0) = 0.5 + \sin(x)$, and periodic boundary conditions. We set $a = 1.23$, $h = 0.01$ and CFL $= 0.123$.

Recall that the unique entropy solution of (21) is smooth up to the critical time $t = 1$. In Figure 1 we plot the convergence rate versus τ at the pre-shock time $t = 0.5$ when the solution is still smooth. These convergence plots have been obtained by computing the approximate convergence rate between two consecutive mesh refinings in the L^2-norm. A log-scale on the x-axis is used.

As expected all the schemes preserve the order of accuracy for both large and small values of τ. Moreover, for the first and third order schemes the accuracy in u component is uniform with respect to τ. On the other hand, a deterioration of the accuracy on the v component is observed for all schemes. We want to point

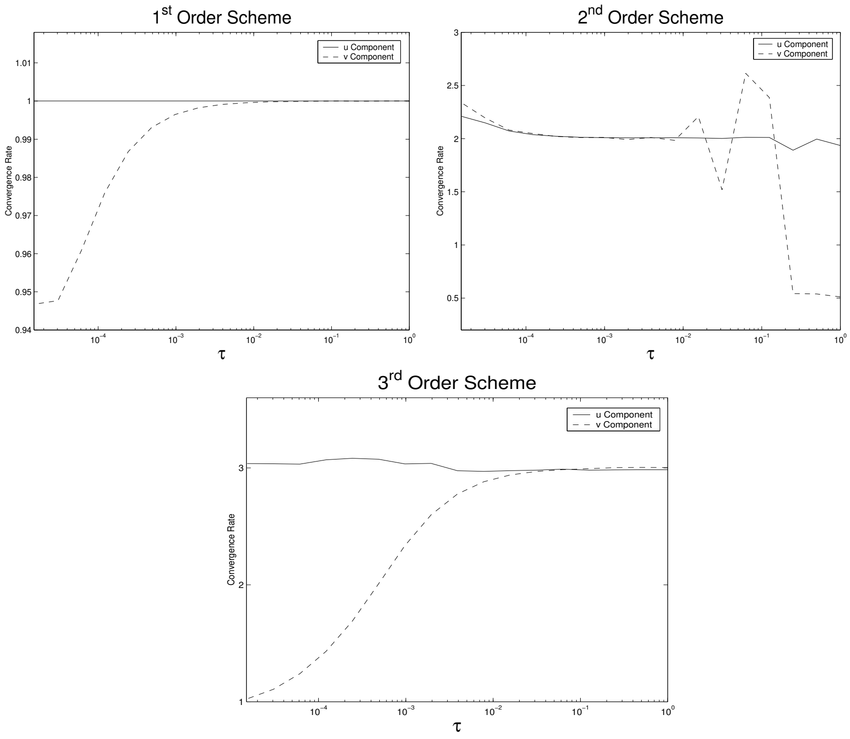

Figure 1: Convergence rates of the relaxation schemes for Burger's equation.

out that we cannot quantify the resolution of the schemes on the v component since an accurate approximation of v can be computed from u in the limit when $\tau \longrightarrow 0$. Remarkably that the third order scheme is more accurate than other schemes.

4.3 One-Dimensional Systems of Hyperbolic Conservation Laws

Here we consider the one-dimensional euler system of gas dynamics,

$$\frac{\partial}{\partial t}\begin{pmatrix} \rho \\ \rho v \\ E \end{pmatrix} + \frac{\partial}{\partial x}\begin{pmatrix} \rho v \\ \rho v^2 + p \\ v(E+p) \end{pmatrix} = 0, \tag{22}$$

or simply

$$\frac{\partial \mathbf{u}}{\partial t} + \frac{\partial}{\partial x}\mathbf{f}(\mathbf{u}) = 0, \tag{23}$$

where $\mathbf{u} := (\rho, \rho v, E)^T$ and $\mathbf{f}(\mathbf{u}) := \big(\rho v, \rho v^2 + p, v(E+p)\big)^T$, where ρ is the density, v is the velocity, ρv is the momentum, E is the energy and p is the pressure. In addition we require the equation of state $p = (\gamma - 1)(E - \frac{1}{2}\rho v^2)$, where the specific heat ratio $\gamma = 1.4$

Based on the formulation (23), a relaxation system can be constructed as in (2) where $\mathbf{A} = \text{diag}\big(a_1, a_2, a_3\big)$. We define the CFL number as in (15). As we

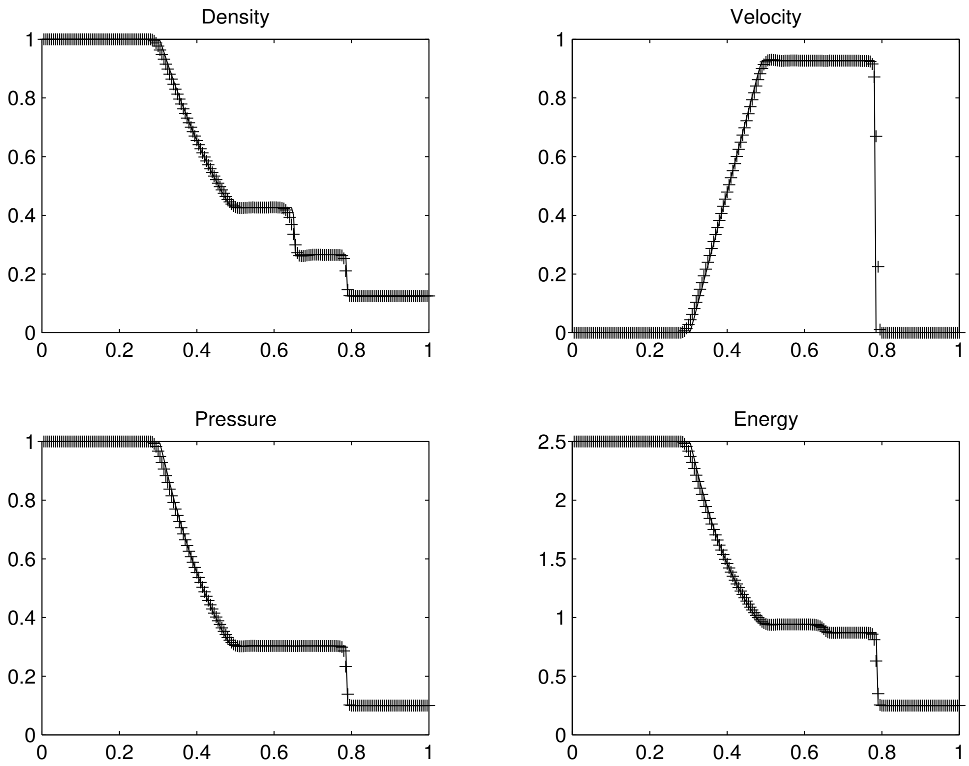

Figure 2: Relaxation results for Sod shock tube test at $t = 0.1644$.

have observed, in the previous examples, that the third order scheme is in all the cases better than other schemes, we present for this example only results performed with third order relaxation scheme using $\tau = 10^{-8}$. The relaxed results are also not included here, because their overlap those obtained by the relaxation schemes. The following test cases are selected.

Sod Shock Tube Test. The first test is the typical Sod shock tube problem. Its solution consists of a left rarefaction, a contact and right shock. It is formulated by the equations (22) augmented by the initial condition

$$\mathbf{u}(x,0) = \begin{cases} (1, 0, 2.5)^T, & \text{if} \quad 0 \leq x < 0.5, \\ (0.125, 0, 0.25)^T, & \text{if} \quad 0.5 \leq x \leq 1. \end{cases}$$

We take $a_1 = 1$, $a_2 = 1.68$, $a_3 = 5.045$, $h = 0.005$ and CFL $= 0.75$. Figure 2 shows the third-order relaxation results with $\tau = 10^{-8}$ at $t = 0.1644$.

Lax Shock Tube Test. Our second test is the Lax shock tube test. It is mathematically formulated by equations (22) subject to the initial data

$$\mathbf{u}(x,0) = \begin{cases} (0.445, 0.311, 8.928)^T, & \text{if} \quad 0 \leq x < 0.5, \\ (0.5, 0, 0.4275)^T, & \text{if} \quad 0.5 \leq x \leq 1. \end{cases}$$

We choose $a_1 = 2.4025$, $a_2 = 11$, $a_3 = 22.2056$, $h = 0.005$ and CFL $= 0.5$. In Figure 3 we present the results obtained by the third-order relaxation scheme with $\tau = 10^{-8}$ at $t = 0.16$.

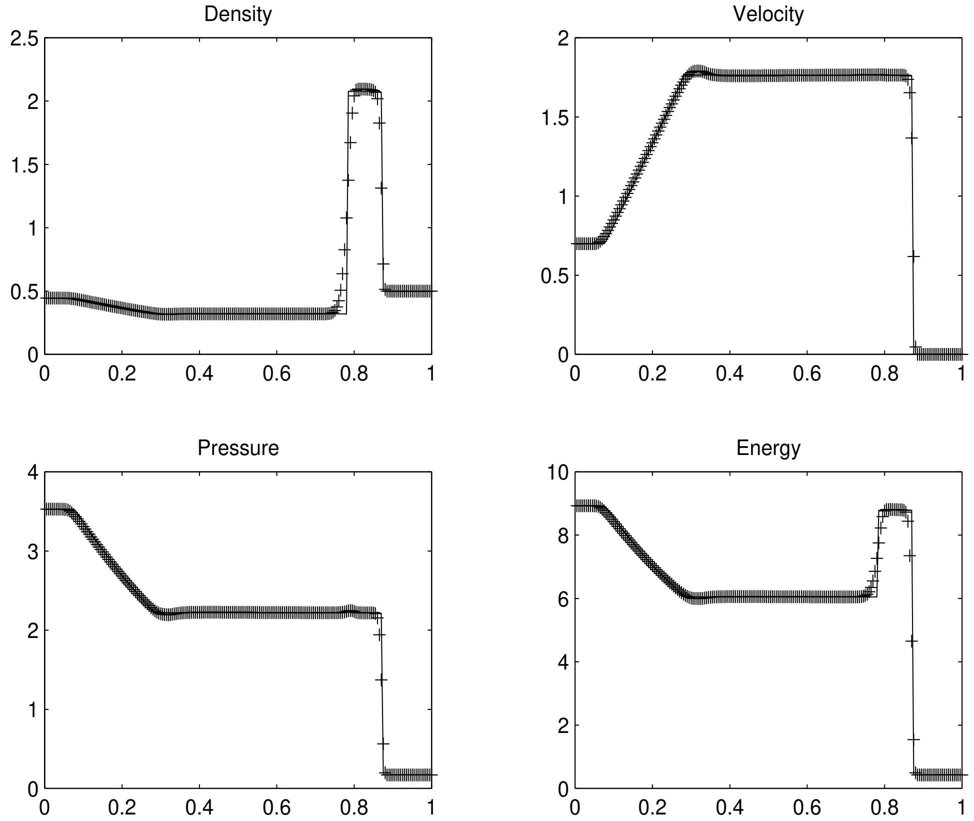

Figure 3: Relaxation results for Lax shock tube test at $t = 0.16$.

Interacting Blast Wave Test. Our final test with Euler equations is the interacting blast wave problem characterised by the initial condition

$$\mathbf{u}(x,0) = \begin{cases} (1,0,2500)^T, & \text{if} \quad 0 \leq x \leq 0.1, \\ (1,0,0.25)^T, & \text{if} \quad 0.1 < x \leq 0.9, \\ (1,0,250)^T, & \text{if} \quad 0.9 < x < 1. \end{cases}$$

We set $a_1 = 32.56$, $a_2 = 169$, $a_3 = 411.8397$, $h = 0.0025$ and CFL $= 0.25$. Results obtained by the third order relaxation scheme with $\tau = 10^{-8}$ at $t = 0.01$ and $t = 0.038$ are shown in Figure 4 and Figure 5, respectively.

The scheme perform very well on the strong shocks in all the examples.

5 Conclusion

We have presented a numerical scheme that is a generalisation for relaxation methods. This scheme is easy to implement and above all no Riemann solvers are necessary. This makes the scheme efficient. However, it is not clear in

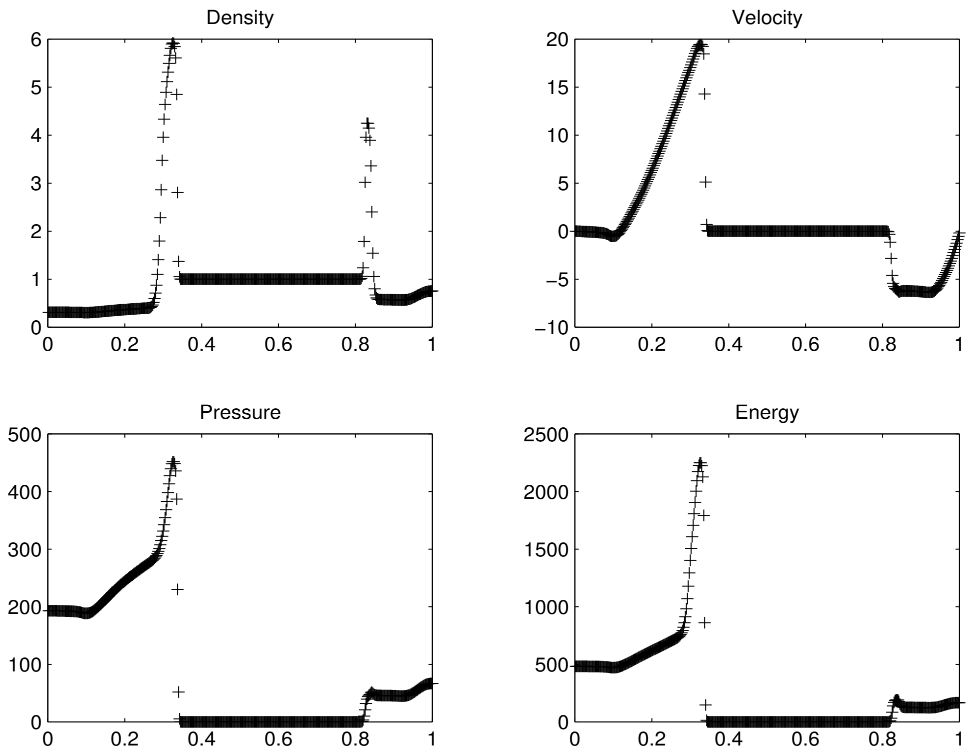

Figure 4: Relaxation results for interacting Blast wave test at $t = 0.01$.

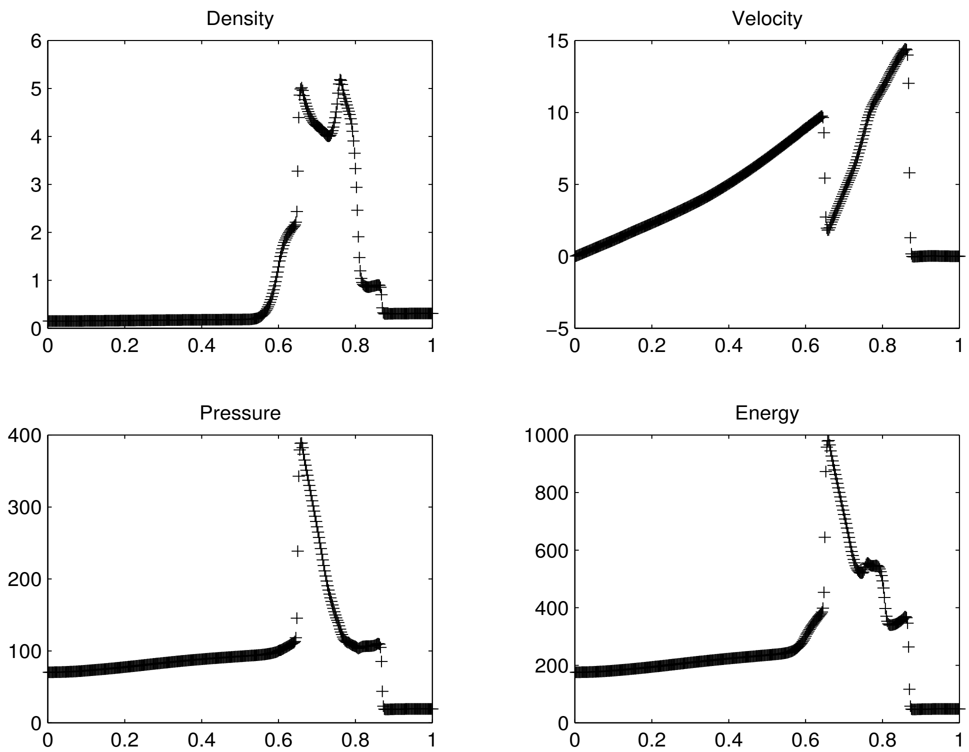

Figure 5: Relaxation results for interacting Blast wave test at $t = 0.038$.

general how one can chose the matrix A^2 in (2). This needs further investigation. On addition work to extend the scheme to multidimensional systems of equations is underway.

Acknowledgements: The authors are deeply grateful to Prof. Axel Klar, for his valuable suggestions and comments.

References

[1] D. Aregba-Driollet and R. Natalini, "Convergence of relaxation scheme for conservation laws," Appl. anal. **61**, 163–193 (1996).

[2] U. Ascher, S. Ruuth and R. Spiteri, "Implicit-explicit Runge-Kutta methods for time-dependent partial differential equations," Appl. Numer. Math. **25**, 151–167 (1997).

[3] M.K. Banda, A. Klar and M. Seaïd, "Lattice-Botzmann type relaxation systems and higher order relaxation schemes for the incompressible Navier-Stokes equation," Submitted.

[4] A. Chalabi, "Convergence of relaxation scheme for hyperbolic conservation laws with stiff source terms," Math. Comput. **68**, 955–970 (1999).

[5] G.Q. Chen, C.D. Levermore and T.P. Liu, "Hyperbolic conservation laws with stiff relaxation terms and entropy," Comm. Pure Appl. Math. **47**, 787–830 (1994).

[6] C.W. Shu and S. Osher, "Efficient Implementation of Essentially Non-Oscillatory Shock-Capturing Schemes," J. Comp. Phys. **77**, 439–471 (1988).

[7] H. Fan, S. Jin and Z. Teng, "Zero Reaction Limit for Hyperbolic Conservation Laws with Source Terms," J. Diff. Equations **168**, 270–294 (2000).

[8] S. Gottlieb, C.W. Shu and E. Tadmor, "Strong Stability-Preserving High-Order Time Discretisation Methods," SIAM Review. **43**, 89–112 (2001).

[9] S. Jin and Z. Xin, "The Relaxation Schemes for Systems of Conservation Laws in Arbitrary Space Dimensions," Comm. Pure Appl. Math. **48**, 235–276 (1995).

[10] S. Jin, "Runge-Kutta Methods for Hyperbolic Systems with Stiff Relaxation Terms," J. Comp. Phys. **122**, 51–67 (1995).

[11] A. Klar, "Relaxation Schemes for a Lattice-Boltzmann type discrete velocity model and numerical Navier-Stokes limit," J. Comp. Phys. **148**, 1–17 (1999).

[12] A. Kurganov and D. Levy, "A third-Order Semi-Discrete Central Scheme for Conservation Laws and Convection-Diffusion Equations," SIAM J. Sci. Comp. **23**, 1461–1488 (2000).

[13] A. Kurganov and E. Tadmor, "New High-Resolution Central Schemes for Nonlinear Conservation Laws and Convection-Diffusion Equations," J. Comp. Phys. **160**, 241–282 (2000).

[14] C. Lattanzio and D. Serre, "Convergence of a relaxation scheme for hyperbolic systems of conservation laws," Numer. Math. **88**, 121–134 (2001).

[15] D. Levy, G. Puppo and G. Russo, "Compact Central Schemes for Multidimensional Conservation Laws," SIAM J. Sci. Comp. **22**, 656–672 (2000).

[16] H.L. Liu and G. Warnecke, "Convergence rates for relaxation schemes approximating conservation laws," SIAM J. Numer. Anal. **37**, 1316–1337 (2000).

[17] R. Natalini, "Convergence to equilibrium for relaxation approximations of conservation laws," Comm. Pure Appl. Math.**49**, 795–823 (1996).

[18] L. Pareschi and G. Russo, "Implicit-Explicit Runge-Kutta Schemes for Stiff Systems of Differential Equations," Preprint.

[19] B. Van Leer, "Towards the Ultimate Conservative Difference Schemes V. A second-Order Sequal to Godunov's Method," J. Comp. Phys. **32**, 101–136 (1979).

[20] W.Q. Xu, "Relaxation limit for piecewise smooth solutions to conservation laws," J. Diff. Eq. **162**, 140–173 (2000).